Growth Instabilities Promote Colony Expansion in Microbial Populations

Alex Gu
Massachusetts Institute of Technology, 77 Massachusetts Ave., Cambridge, MA 02139-4307
(Dated: May 17, 2025)

Microbial colonies exhibit diverse morphologies influenced by environmental conditions, but how these patterns affect population dynamics remains poorly understood. We investigate a diffusion-reaction model of colonial growth, focusing on the links between growth instabilities, demographic noise, and expansion velocity. Through numerical simulations, we demonstrate that instabilities quite generally accelerate colony growth: increasing demographic noise and decreasing lateral diffusion both promote faster expansion, but only in the unstable growth regime. By systematically varying parameters that control instability without directly affecting planar front propagation, we provide strong evidence that fingering patterns provide a competitive advantage by increasing nutrient access. These results reveal an important mechanism by which spatial structure influences microbial population dynamics and evolution.

I. INTRODUCTION

Microbial populations in nature rarely grow in well-mixed environments, instead forming spatially structured colonies with complex morphologies that can profoundly influence their ecological and evolutionary dynamics [1]. These spatial patterns may emerge, for example, from the interplay between nutrient diffusion, biomass growth, and cell motility, resulting in growth fronts that can transition between smooth, stable expansion and irregular, fingering instabilities [2, 3]. The morphological transitions in microbial colonies bear striking resemblance to pattern formation phenomena observed in other physical systems, such as viscous fingering and dendritic growth [4]. However, the nature of these instabilities can be quite complex, and while there have been developments towards a mathematical description of certain systems [3], the instability phenomena and their functional consequences for microbial growth and competition remain incompletely understood.

In a previous study [5], we found a counterintuitive relationship between demographic noise and colony expansion: under certain conditions, increased stochastic fluctuations actually accelerated front propagation. This observation contradicts the typical expectation from reaction-diffusion systems, where noise generally slows front propagation by disrupting the coherent growth at the leading edge [6]. We hypothesized that this acceleration was linked specifically to the fingering instabilities that emerge in particular parameter regimes, where fluctuations might trigger beneficial pattern formation rather than simply disrupting growth.

The possibility that growth instabilities might enhance rather than impede colony expansion has significant implications for understanding microbial ecology and evolution in spatially structured environments. If unstable growth patterns enable faster resource utilization and territorial expansion, then the conditions that promote such instabilities could provide selective advantages to microbial populations or subpopulations capable of inducing them.

In this work, we systematically investigate this hypothesis by examining multiple parameters that induce growth instabilities and carefully analyzing their effects on colony expansion velocity. We focus on three key parameters: demographic noise, the motility exponent that governs density-dependent diffusion, and the ratio of lateral to forward diffusion in an anisotropic extension of the model. By manipulating these parameters independently, we can isolate the specific effects of growth instabilities from other factors that directly influence expansion velocity. The resulting framework allows us to characterize the phase transitions between stable and unstable growth regimes and to quantify the functional consequences of these transitions for colony expansion.

II. MODEL

A. Reaction-Diffusion Model

Following previous work [2, 3, 5], we model microbial colony growth using coupled reaction-diffusion equations for biomass and nutrient fields. This continuum approach represents the colony as a density field $b(x, y, t)$ that grows by consuming a nutrient field $n(x, y, t)$. The basic dynamics incorporate four key processes: nutrient diffusion, biomass diffusion, nutrient consumption, and biomass growth, which can be represented by the following diffusion-reaction equations:

$$\begin{aligned} \frac{\partial b}{\partial t} &= \nabla^2 \left[\frac{D_b}{\kappa + 1} b^\kappa b \right] + \gamma n b + \sqrt{\gamma n b \Delta b}\,\eta, \\ \frac{\partial n}{\partial t} &= D_n \nabla^2 n - \gamma n b - \sqrt{\gamma n b \Delta b}\,\eta, \end{aligned} \tag{1}$$

where D_b is the biomass diffusion constant, D_n is the nutrient diffusion constant, γ is the nutrient uptake rate, and κ is the motility exponent that determines how diffusion depends on cell density. The noise terms represent demographic fluctuations, with Δb controlling noise strength. The first term in the biomass equation describes a density-dependent diffusion process that plays an important role in determining colony morphology. When $\kappa = 0$, this reduces to standard Fickian diffusion, while for $\kappa > 0$, the diffusion coefficient increases with density, producing cooperative biomass movement. This cooperative effect has been observed in certaub bacterial species, where cells can exert mechanical forces on their neighbors (e.g. through direct contact) [7].

A key feature of this model is its transition between stable and unstable growth regimes. Intuitively, the stability boundary represents a balance between two competing processes: (1) lateral diffusion of biomass along the front, which tends to smooth out irregularities, and (2) enhanced growth at protrusions that extend into nutrient-rich regions, which amplifies irregularities. When biomass diffusion dominates, the front remains stable and smooth. When nutrient diffusion and local growth dominate, small perturbations can grow into finger-like projections. A linear stability analysis identifies a dimensionless parameter $D = \frac{D_b n_0^\kappa}{D_n}$ that largely controls this transition [3]. When $D \gtrsim 1$, growth is generally stable, while for $D \lesssim 1$, the front becomes unstable to perturbations with sufficiently long wavelengths. Importantly, the value of κ and other parameters modify this transition, with higher values of κ making the system more prone to instabilities.

In our previous work [5], we demonstrated that these fingering instabilities significantly affect not only colony morphology but also competitive dynamics between different phenotypes. Specifically, we found that in the unstable growth regime, phenotypes with higher demographic noise (Δb) gained a competitive advantage, contrary to expectations from classical population dynamics theory.

For the present study, we extend the model to include anisotropic biomass diffusion, with potentially different diffusion coefficients in the direction of front propagation (x-direction) and laterally along the front (y-direction). This modification leads to the biomass diffusion term:

$$\nabla^2 \left[\frac{D_b}{\kappa+1} b^\kappa b \right] \rightarrow \frac{\partial}{\partial x} \left[\frac{D_{b,x}}{\kappa+1} b^\kappa \frac{\partial b}{\partial x} \right] + \frac{\partial}{\partial y} \left[\frac{D_{b,y}}{\kappa+1} b^\kappa \frac{\partial b}{\partial y} \right] \tag{2}$$

This anisotropic model introduces a new parameter $r = \frac{D_{b,y}}{D_{b,x}}$ representing the ratio of lateral to forward diffusion. This parameter allows us to induce instabilities in a manner that doesn't directly affect the baseline velocity of a planar front, which depends primarily on diffusion in the propagation direction.

The key dimensionless parameters that govern the system behavior are now:

$$D = \frac{D_{b,x} n_0^\kappa}{D_n}, \quad \sigma = \frac{\gamma \Delta b}{D_n}, \quad r = \frac{D_{b,y}}{D_{b,x}}, \quad \kappa \tag{3}$$

where D controls the baseline stability, σ determines the strength of demographic fluctuations, r represents diffusion anisotropy, and κ is the motility exponent that modifies how instabilities form and propagate.

B. Numerical Implementation

To investigate the dynamics of this model, we perform extensive numerical simulations, building on techniques developed in [2, 5]. The simulations are conducted on a two-dimensional rectangular domain with periodic boundary conditions in the lateral (y) direction and hard-wall boundary conditions at the top and bottom in the propagation (x) direction. We initialize each simulation with a thin line of biomass at the bottom boundary and a uniform nutrient concentration n_0 throughout the domain, then allow the system to evolve according to the stochastic reaction-diffusion equations. To discretize the dynamics, we employ spatial lattice spacings of dx, dy and adaptive time steps chosen to ensure numerical stability:

$$dt = \frac{1}{10} \min \left(\frac{dxdy}{D_n}, \frac{dxdy}{D_{b,x} n_0^\kappa}, \frac{dxdy}{D_{b,y} n_0^\kappa}, \frac{1}{\gamma n_0} \right) \tag{4}$$

The demographic noise terms are implemented by modeling biomass growth as a random sampling from a beta distribution taken to match the mean and variance of the growth step, which provides a continuous and bounded representation of the noise. Also, we implement a cessation of biomass motility when the local nutrient concentration falls below a critical threshold $n_c = 1$, which primarily affects the interior of the colony where nutrients have been depleted, while allowing continued expansion at the nutrient-rich front.

To quantify the properties of the growing colony, we define the front properties are follows: The front position is identified by finding, for each y-coordinate, the x-value where the product of biomass and nutrient $(b \cdot n)$ reaches its maximum, correponding the point of maximum growth. The front velocity is calculated by measuring the time required for the total biomass to reach 40% and 80% of the theoretical maximum (determined by conservation of mass), which excludes both initial transients and potential boundary effects at later stages. The front roughness $w^2 = \frac{1}{L} \int [h(t,x) - \bar{h}(x)]^2 dx$ is quantified as the variance of front positions across the entire width of the simulation domain, with values below one grid cell set to zero.

Our simulations were run with $N_x = 125, N_y = 200, n_0 = 100, n_c = 1, dx = dy = 0.025$.

III. RESULTS

A. Effects of Demographic Noise σ

We previously observed that demographic noise accelerates front propagation in unstable colonies [5]; we

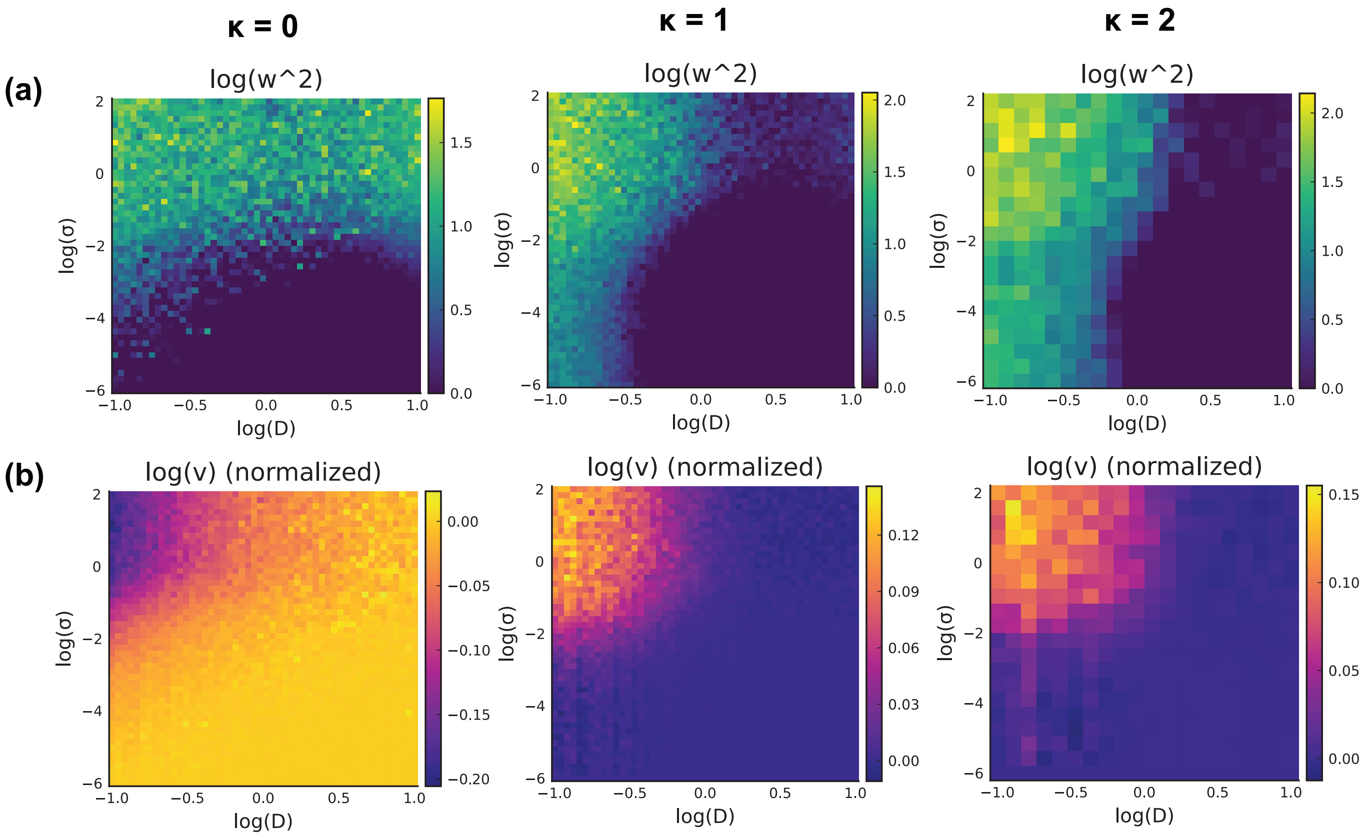

FIG. 1: Heatmaps showing (a) roughness w^2 and (b) normalized front velocity v for varying D and σ with $\kappa = 0, 1, 2$. For each D, velocities are normalized to the value at minimum σ. The roughness heatmap reveals the phase boundary between stable (roughness $= 0$) and unstable growth, while the velocity heatmap shows that increased noise accelerates front propagation in the unstable regime ($\kappa = 1, 2$) but not in the $\kappa = 0$ case.

now characterize this effect more completely. Fig. 1 presents heatmaps of front roughness and normalized velocity across the parameter space of diffusion ratio D and noise strength σ for different values of the motility exponent κ. The roughness heatmaps (Fig. 1a) effectively map out the phase diagram of the system, with the boundary where roughness becomes non-zero marking the transition from stable to unstable growth. The velocity heatmaps (Fig. 1b) reveal a striking pattern: for $\kappa = 1$ and $\kappa = 2$, regions of instability correspond closely to regions of enhanced velocity. As σ increases and destabilizes the front, we observe a corresponding increase in normalized velocity. In contrast, for $\kappa = 0$, increased noise leads to roughness but decreases front velocity rather than enhancing it. This aligns with theoretical predictions that true fingering instabilities occur only for $\kappa > 0$ [3], while the roughness at $\kappa = 0$ represents noise-induced fluctuations rather than self-amplifying patterns.

These results provide strong evidence that fingering instabilities specifically—not just any form of front roughness—can promote faster colony expansion. The enhanced velocity appears to be an intrinsic feature of the nonlinear dynamics of fingering patterns, where protrusions into nutrient-rich regions experience accelerated growth.

B. Effects of Motility Exponent κ

To further investigate how the motility exponent κ influences colony expansion, we systematically vary κ and the diffusion ratio D while keeping noise strength low ($\sigma = 0.0001$). Figure 2 presents the resulting phase diagram and velocity scaling relationships.

The roughness heatmap (Fig. 2a) reveals how the stability boundary depends on both D and κ. This produces a stability phase diagram that reproduces the theoretical predictions from [3] of a critical transition D_c that is *linear* in κ. However, we observe some quantitative differences in the exact position and slope of the transition boundary compared to the analytical predictions due to the linear stability analysis. As discussed in [3], these discrepancies likely result from finite-size effects in our simulations, as the domain size may be smaller than some relevant wavelengths of the instability, biasing the system toward stability. Figure 2b depicts the front velocity dependence on D and κ, which agrees qualitatively

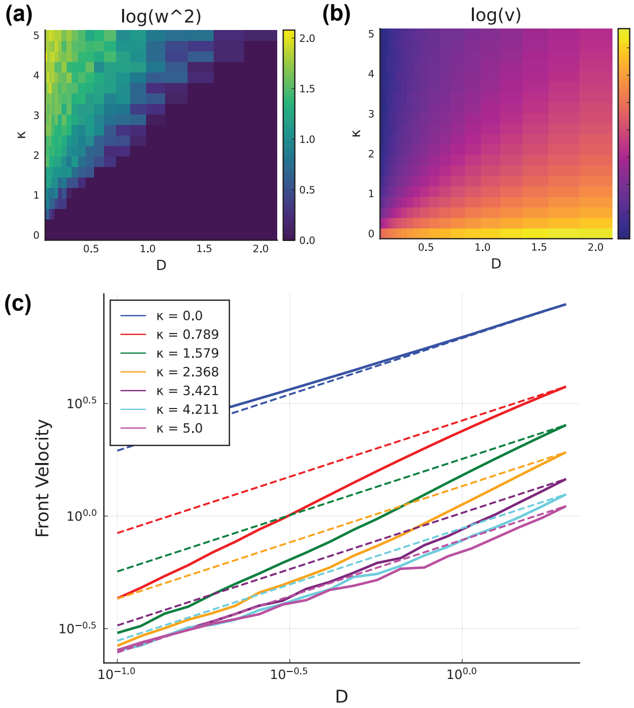

FIG. 2: (a) Heatmap of log roughness for D vs κ showing the stability phase boundary. (b) Heatmap of log velocity for D vs κ. (c) Log-log plot of velocity vs D for various κ values. The dotted line shows $v \propto \sqrt{D}$ scaling expected for standard diffusion, scaled to match the data at the largest D value. As D decreases, higher κ values show earlier and stronger deviation from this scaling, suggesting an increase in velocity due to the onset of instabilities.

with the analysis due to [3] (Fig. 1), showing that front velocity generally decreases with increasing κ.

Figure 2c presents a log-log plot of front velocity versus diffusion ratio D for different κ values. At large D, where growth is stable and planar regardless of κ, velocity closely follows the standard diffusion scaling $v \propto \sqrt{D}$. This scaling relationship is expected from the classic Fisher wave behavior, where front velocity in a reaction-diffusion system scales with the square root of the diffusion coefficient. As D decreases and approaches the instability threshold, velocity begins to deviate from this standard scaling, exceeding the predicted values. This deviation occurs earlier (at higher D values) for larger κ values, corresponding to the earlier onset of instabilities seen in the phase diagram. For $\kappa = 5$, for example, the deviation is substantial even at relatively high D values, while for $\kappa = 0$, where true fingering instabilities do not occur, the deviation is minimal. This systematic relationship between instability onset and enhanced velocity provides compelling evidence that the instabilities themselves accelerate front propagation beyond what would be expected for stable growth.

C. Effects of Anisotropic Diffusion

To more conclusively demonstrate that instabilities directly promote colony growth, we examine the effects of anisotropic diffusion by varying the diffusion coefficients in the propagation direction ($D_{b,x}$) and lateral direction ($D_{b,y}$) independently. This approach offers a crucial advantage: in planar front propagation, velocity depends primarily on diffusion in the propagation direction, not on lateral diffusion. Thus, any effects of reduced lateral diffusion on velocity must result from the instabilities it induces rather than from direct effects on the biomass movement.

Figure 3 presents heatmaps showing how roughness and normalized front velocity vary with D_x and D_y for different κ values, maintaining low background noise ($\sigma = 0.0001$). We note that the apparent artifacts in the bottom right and top left corners of the $\kappa = 1, 2$ heatmaps of 3(b) are purely due to limitations of the simulation method and are not physical.

The roughness heatmaps (Fig. 3a) clearly demonstrate the phase transition to instability as lateral diffusion (D_y) decreases relative to forward diffusion (D_x). For $\kappa = 1$ and $\kappa = 2$, this transition exhibits a relatively sharp boundary, while for $\kappa = 0$, the transition less well-defined. Interestingly, the critical value of D_y for instability onset does not vary strongly with D_x and shows a potentially non-monotonic relationship, particularly for $\kappa = 1$. The velocity heatmaps (Fig. 3b) provide the perhaps most direct evidence yet for our central hypothesis. For $\kappa = 1$ and $\kappa = 2$, regions of instability correspond strongly to regions of enhanced velocity. As lateral diffusion decreases and triggers fingering patterns, front velocity increases significantly compared to the planar front case. In contrast, for $\kappa = 0$, reduced lateral diffusion has minimal effect on velocity despite inducing roughness. This pattern matches our findings for noise-induced instabilities and strongly supports the conclusion that true fingering instabilities promote colony growth. The velocity enhancement cannot be explained simply by the redistribution of biomass diffusion from lateral to forward movement, as such an effect would appear regardless of κ value. Instead, the enhanced growth appears to be an intrinsic property of the fingering patterns themselves, which emerge only for positive κ values.

The anisotropic diffusion experiments provide particularly compelling evidence because they isolate the effect of instabilities from other factors that directly affect planar front propagation. By keeping the forward diffusion coefficient constant while varying only lateral diffusion, we demonstrate that the instability itself—not just changes in diffusion rates—drives the increased expansion velocity.

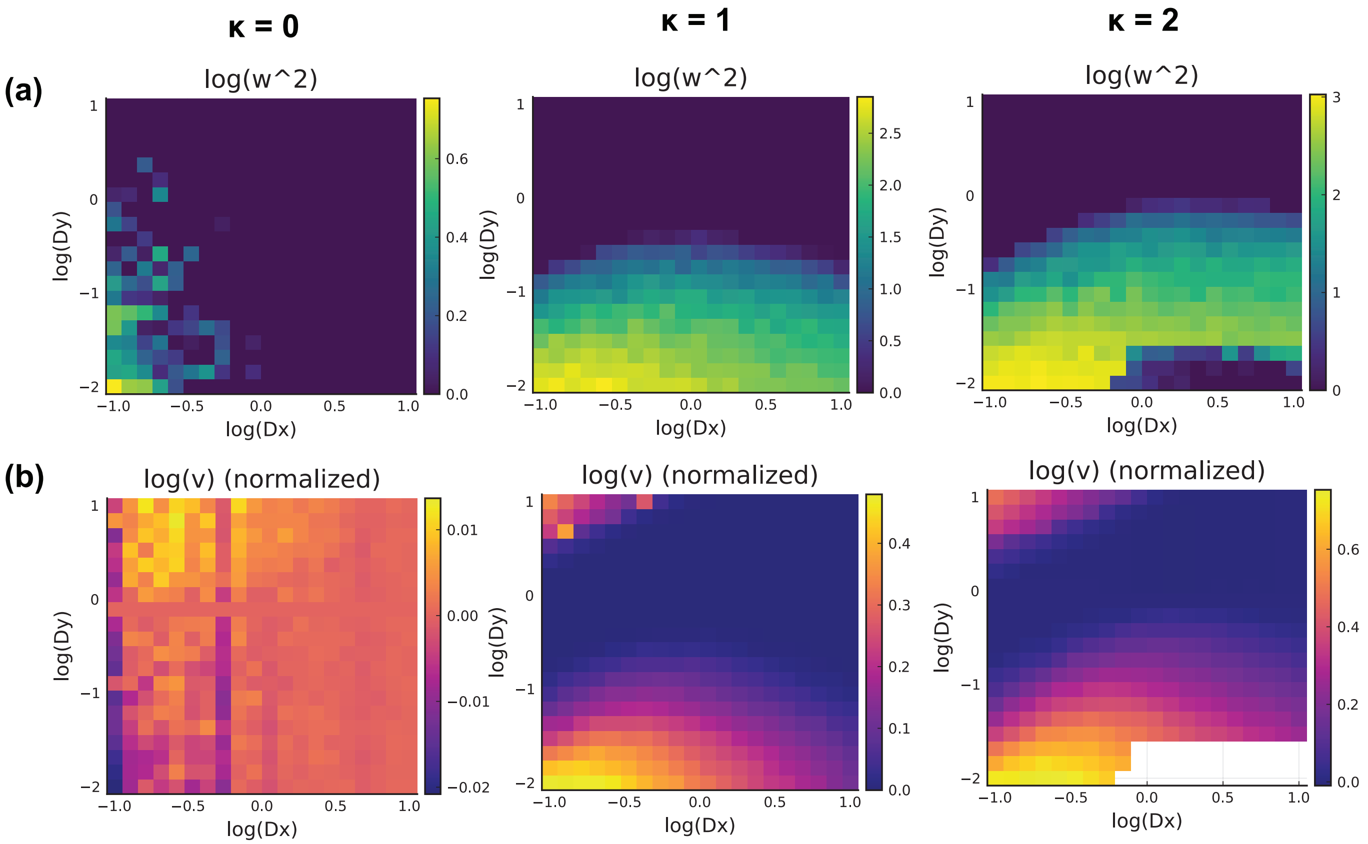

FIG. 3: Heatmaps showing (a) roughness and (b) normalized front velocity for varying D_x and D_y with $\kappa = 0, 1, 2$. For each D_x, velocities are normalized to the value at maximum D_y. The roughness maps reveal a clear phase transition as lateral diffusion decreases, while velocity maps show corresponding acceleration only for $\kappa > 0$. Artifacts in the bottom right and top left corners of the $\kappa = 1, 2$ heatmaps of (b) are purely due to limitations of the simulation method and are not physical.

IV. DISCUSSION

Our results demonstrate a consistent and remarkable pattern: growth instabilities significantly enhance the expansion velocity of microbial colonies, but only when these instabilities take the form of true fingering patterns rather than simple noise-induced front roughness. This enhancement occurs specifically in parameter regimes supporting fingering instabilities ($\kappa > 0$, $D < 1$), and becomes more pronounced as the instabilities become more extreme.

The mechanism behind this enhancement likely involves the fingering pattern's ability to access higher nutrient concentrations beyond the average position of the front. Once a finger forms, it experiences a steeper nutrient gradient than would be present at a planar front, leading to accelerated growth. This creates a positive feedback loop where the fastest-growing protrusions advance further into nutrient-rich territories, enhancing their growth advantage and accelerating the overall front velocity.

Our finding that demographic noise can trigger growth-enhancing instabilities has particularly interesting implications for population biology. Traditional models often treat demographic stochasticity as a disruptive force that reduces growth efficiency. Our results suggest that in spatially structured populations, demographic noise can actually enhance growth through pattern formation, providing a potential selective advantage. Similarly, the dependence of growth enhancement on the motility exponent κ suggests that cooperative cell movement—where cellular motility increases with density—could provide advantages beyond simple resource exploration. By promoting instabilities that accelerate colony expansion, cooperative motility may enable more efficient resource exploitation in spatially structured environments.

These findings have important implications for understanding microbial ecology and evolution. First, they suggest that conditions promoting instabilities may confer growth advantages beyond what would be predicted from well-mixed population models. Second, they indicate that the spatial structure of microbial populations is not merely a consequence of growth dynamics but can actively influence those dynamics. Finally, they suggest that evolutionary selection in spatially structured environments might favor traits that induce beneficial instabilities under appropriate conditions.

Future work should focus on experimental validation of these computational predictions, perhaps by manipulating factors that control front stability in model microbial systems and measuring resulting growth rates, as well as further developing a complete analytical understanding of the effects of instability and the associated phase transition.

V. ACKNOWLEDGMENTS

I would like to acknowledge my UROP mentor Daniel Swartz for his consistent support and mentorship throughout this project. I would also like to thank Kirill S. Korolev for a useful and insightful discussion.

---

[1] D. Yanni, P. Márquez-Zacarías, P. J. Yunker, and W. C. Ratcliff, "Drivers of spatial structure in social microbial communities," *Current Biology*, vol. 29, no. 11, pp. R545–R550, 2019.
[2] A. Golden, I. Dukovski, D. Segrè, and K. S. Korolev, "Growth instabilities shape morphology and genetic diversity of microbial colonies," *Physical Biology*, vol. 19, p. 056005, aug 2022.
[3] J. Müller and W. van Saarloos, "Morphological instability and dynamics of fronts in bacterial growth models with nonlinear diffusion," *Phys. Rev. E*, vol. 65, p. 061111, Jun 2002.
[4] J. S. Langer, "Dendrites, viscous fingers, and the theory of pattern formation," *Science*, vol. 243, pp. 1150–1156, mar 1989.
[5] A. Gu, "Growth instabilities shape competitive dynamics and front propagation in microbial colonies," *Unpublished manuscript*, 2024.
[6] C. Mueller, L. Mytnik, and J. Quastel, "Effect of noise on front propagation in reaction-diffusion equations of kpp type," 2009.
[7] I. Golding, Y. Kozlovsky, I. Cohen, and E. Ben-Jacob, "Studies of bacterial branching growth using reaction–diffusion models for colonial development," *Physica A: Statistical Mechanics and its Applications*, vol. 260, no. 3, pp. 510–554, 1998.